PHYSICAL REVIEW C VOLUME 26, NUMBER 6 DECEMBER 1982

Inclusive proton reactions at 164 MeV

R. E. Segel, T. Chen,* and L. L. Rutledge, Jr.†
Northwestern University, Evanston, Illinois 60201

J. V. Maher
University of Pittsburgh, Pittsburgh, Pennsylvania 15260

John Wiggins and P. P. Singh
Indiana University, Bloomington, Indiana 47405

P. T. Debevec
University of Illinois, Urbana, Illinois 61801
(Received 2 April 1982)

Singles proton, deuteron, triton, ^{3}He, and alpha spectra resulting from the bombardment of ^{27}Al, ^{58}Ni, ^{62}Ni, and ^{208}Pb targets were measured. Data were taken over the angular range 25°—150°. Most of the data were taken at a bombarding energy of 164 MeV; some data were taken at 100 MeV. The ratios of fast (>30 MeV) particle yields are $p:d:t:{}^3\text{He}:\alpha \approx 100:10:1:1:1$. The deuteron spectra fall off more sharply with exit particle energy than do the proton spectra while tritons fall still more sharply, and the fast ^{3}He and α spectra are similar in shape to the triton spectra. Fast particle angular distributions are all forward peaked with the forward peaking increasing with increasing outgoing particle energy. Angular distributions for the different particle species are quite similar and shapes of both spectral and angular distributions are rather independent of target. Proton and alpha evaporation peaks are prominent, deuterons less so, and evaporation peaks are not apparent in the triton and ^{3}He spectra.

[NUCLEAR REACTIONS 164, 100 MeV p on ^{27}Al, ^{58}Ni, ^{62}Ni, ^{208}Pb; measured outgoing p, d, t, ^{3}He, α spectra; $25° \leq \theta \leq 150°$.]

I. INTRODUCTION

With the present generation of intermediate energy accelerators it is possible to study proton induced nuclear reactions in an energy region where little has been done previously. While it is true that proton beams in the 100—200 MeV range have been available for at least three decades, it was only recently that beams of sufficient quality were produced for it to be possible to do experiments in this region with anything like the completeness and precision that nuclear physicists have become used to when working at lower energies.

An incident projectile in the 50—200 MeV range can dislodge inner nucleons, and thus parts of the nucleus can be studied that are not accessible at lower energies, where the reactions are dominated by interaction with the valence nucleons. On the other hand, these energies are below the pion production threshold and therefore it should be possible to interpret the experimental results in terms of nucleon-nucleon collisions within a nucleus. Thus, a rich field for nuclear physics studies may well exist in this previously rather unexplored energy region. A first step towards unraveling the mechanisms which govern reactions in this energy region is to look at reaction products which result from such interactions.

This experiment was performed at the Indiana University Cyclotron Facility. Proton, deuteron, triton, ^{3}He, and alpha particle spectra were obtained at a number of angles between 25° and 150° with ^{27}Al, ^{58}Ni, ^{62}Ni, and ^{208}Pb targets. Most of the data were taken at 164 MeV; some data were also taken at 100 MeV. Fragmentary data on the production of heavier ions were also obtained. It has already

TABLE I. Summary of runs.

Target	Thickness	$E_p = 165$ MeV	$E_p = 100$ MeV
^{208}Pb	7.72 mg/cm^2	25°, 30°, 40°, 60°, 90°, 120°, 150°	30°, 90°
^{62}Ni	1.90 mg/cm^2	25°, 30°, 40°, 50°, 60° 80°, 90°, 100°, 110°, 120°, 130°, 140°, 150°	30° 40°, 60°, 90° 90°, 120°, 150°
^{58}Ni	2.54 mg/cm^2	25°, 30°, 40°, 60°, 90°, 120°, 150°	30°, 40° 90°, 120°
^{27}Al	1.96 mg/cm^2	25°, 30°, 40°, 60°, 90°, 120°, 150°	

been reported[1] that the proton spectra in the present data show considerably less peaking due to quasi-free nucleon-nucleon scattering than had been previously reported.[2]

II. EXPERIMENTAL SETUP

The experiments were conducted in the 162 cm scattering chamber that has been installed at the Indiana cyclotron for low resolution charged particle experiments. Table I lists the targets and gives their thicknesses, which were determined by measuring the energy loss for alpha particles from a radioactive source. The incident beam lost a negligible amount of energy in traversing the target. Beam current varied between 5 and 200 nA and was limited by the counting rate in the detectors. Energies and angles at which data were taken are also given in Table I. Slit scattering, not noticed until after the experiment was completed, rendered some of the 150° data invalid.

The target was viewed by two counter telescopes. One telescope consisted of a 1000 μm thick silicon detector backed by a 7.6 cm thick NaI(Tl) crystal, which is a thickness sufficient to stop the highest possible energy protons. For particles whose energy was measured by the NaI(Tl) crystal, a correction was made for the energy lost in the dead layer in front of the crystal. The other telescope consisted of three surface barrier detectors, 50, 1000, and 5000 μm thick, respectively, backed by a veto detector. Since the energy loss for reaction products was considerably greater in the first detector than in the target, it was primarily the thickness of the first detector that determined the low energy cutoff. This cutoff was about 2.5 MeV for protons, 3 MeV for deuterons, 3.5 MeV for tritons, 7 MeV for ^{3}He, and 8 MeV for ^{4}He. During one run a 25 μm thick detector was placed in front of the second telescope to allow the detection of heavy ions.

The proton, deuteron, and triton spectra were corrected for nuclear interactions in the NaI(Tl) detector.[3] Since the data needed to make this correction apparently only exist for protons, the same correction formula was used for the deuteron and the triton spectra as was used for the protons. While the interaction cross sections for the heavier particles are greater, their range is smaller, and therefore, this procedure is probably acceptable. The ranges of the $Z=2$ particles were so small that nuclear interaction corrections were unnecesary.

For much of the ^{62}Ni and ^{208}Pb and all of the ^{27}Al 164 MeV data the 5000 μm detector was missing, resulting in a gap in the spectra corresponding to particles with a range greater than 1050 μm of Si but still not energetic enough to pass through the ≈ 1 g/cm^2 dead layer in front of the NaI(Tl) crystal. After the 5000 μm detector was put in, ^{62}Ni was rerun at 25°, 60°, and 150° and ^{208}Pb was rerun at 25° and at 60°. These data, and the fact that the shapes of the fast particle spectra were nearly the same for all targets, were used in estimating the amount of cross section lost in the gap. From the systematics, an estimate was made of the missing cross sections in the ^{27}Al spectra.

Absolute cross sections for the various targets were determined in a separate run at 165 MeV. In this run the p-p cross section was measured at several angles and the results agreed to within about 15% with the well established values,[4] with the relative cross sections agreeing to within 5%. At the 100 MeV bombarding energy the ^{58}Ni results were in good agreement with those obtained by Wu,

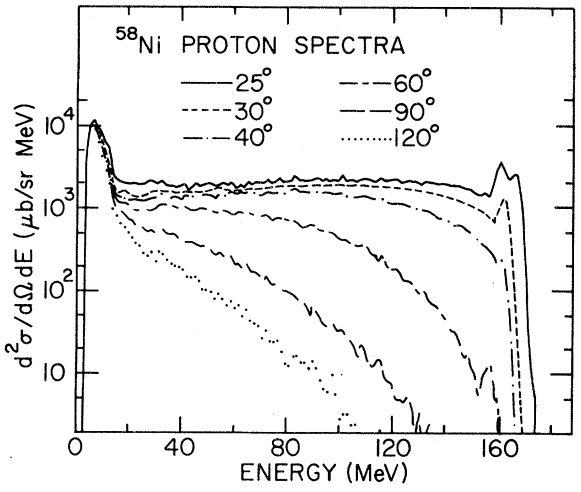

FIG. 1. Proton spectra at the various angles from bombarding a ^{58}Ni target with 164 MeV protons.

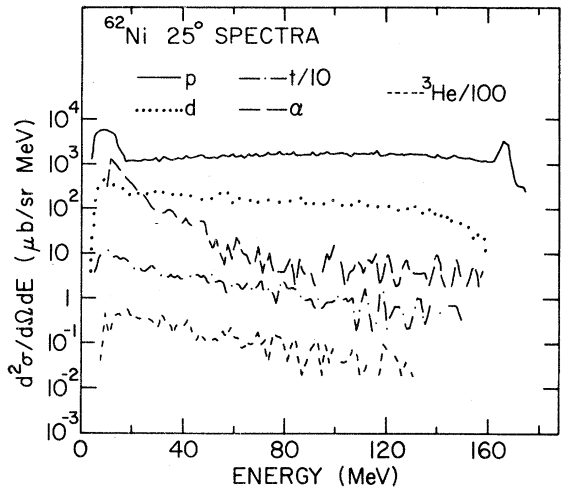

FIG. 3. Spectra of various particles at 25° from a ^{62}Ni target.

Chang, and Holmgren[5] with this target at this energy.

III. EXPERIMENTAL RESULTS

Overall, the spectra are characterized by a low energy peak, attributable to evaporation, and a fast portion whose intensity decreases sharply with increasing angle. Proton spectra at various angles from one target, ^{58}Ni, are shown in Fig. 1 (unless otherwise stated the incident energy was 164 MeV). Proton spectra from the four targets at 25° and 120° are shown in Fig. 2. Figure 3 shows the spectra at 25° from a ^{62}Ni target for all five detected particles.

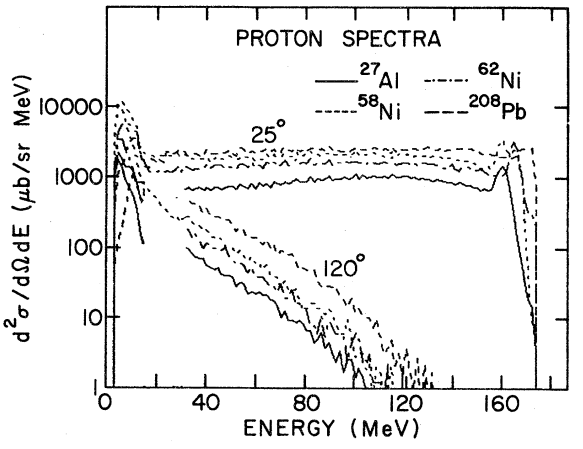

FIG. 2. Proton spectra at 25° and at 120° from the various targets. The gap in some of the spectra was caused by protons stopping in the dead layer in front of the NaI(Tl) crystal. When the other spectra were taken the second telescope was thick enough to cover this gap.

Triton spectra at 25° and at 120° are displayed in Fig. 4. Proton spectra at 30° from a ^{58}Ni target at the two bombarding energies are given in Fig. 5 along with the similar comparison of deuterons at 60° from a ^{62}Ni target. At the smallest angles an elastic peak is present in the proton spectra and at these angles all of the particles are produced in measurable quantities up to nearly the maximum possible energy. The evaporation peak is sometimes not evident at the more forward angles but there always is a low energy peak at angles of 90° or more. Protons and alpha particles are most strongly evaporated and the evaporation peak is most prominent in these spectra. At forward angles the low energy alpha peak is very broad and it is not possible to make a clean distinction between fast and evapora-

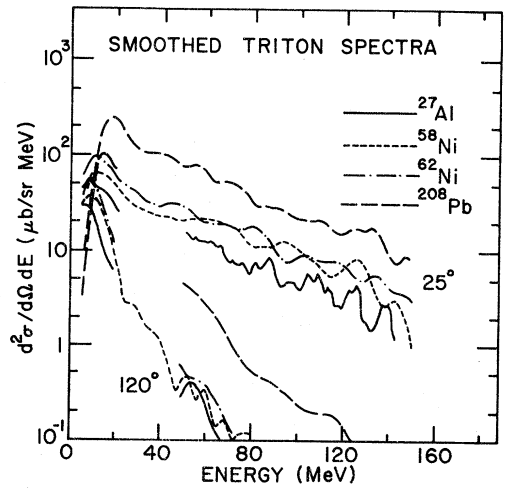

FIG. 4. Trition spectra at 25° and 120° from the various targets. The spectra have been smoothed.

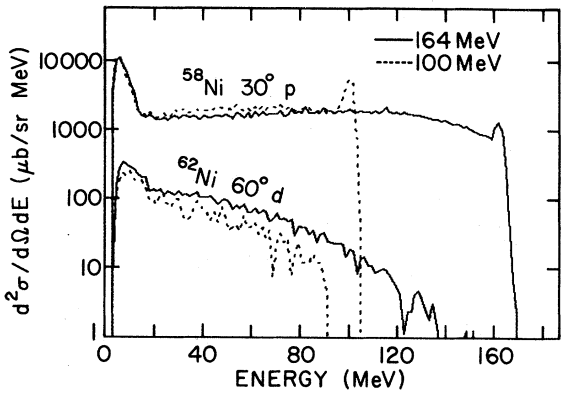

FIG. 5. Proton spectra at 30° from a ^{58}Ni target and deuteron spectra at 60° from ^{62}Ni at bombarding energies of 100 and 164 MeV.

tion particles. A reasonably distinct low energy peak is usually present in the deuteron spectra, at least at backward angles. However, for ^{3}H and ^{3}He, one can only say that the yield decreases with increasing angle, with the falloff greater the greater the energy, until at backward angles the yield is concentrated in the evaporation region.

Broad peaks, which could be indicative of quasifree proton-nucleon scattering, are present at forward angles in the proton spectra, but it is clear that quasifree peaks do not dominate the proton spectra at any of the angles at which measurements were made. The extent to which quasifree peaks are observed in these and other spectra taken in the 100–800 MeV region has been discussed elsewhere.[1] Intermediate energy proton inelastic scattering differs from electron[6] and pion[7] inelastic scattering in that in the latter two cases the inclusive spectra are dominated by quasifree peaks. At the forward angles the ^{27}Al proton spectra show a somewhat larger maximum in the region where quasifree scattering is expected than do the heavier targets. Outside of this the shapes of the fast proton spectra are rather independent of target. From Fig. 2, it is clear that the yield of fast protons is a more rapidly varying function of A in the backward direction than it is in the forward direction with the yield of fast protons varying as about $A^{0.5}$ at 25° and $A^{0.8}$ at 120°. The $\approx$40% difference between ^{58}Ni and ^{62}Ni is on the borderline of significance in view of the estimated $\pm$15% experimental uncertainty. Angular distributions of the protons from ^{58}Ni, binned in various energy regions, are shown in Fig. 6. As expected, the higher the exiting proton energy the more rapidly the yield falls off with angle. The lowest energy bin, 0–30 MeV, is dominated by the nearly isotropic evaporation peak.

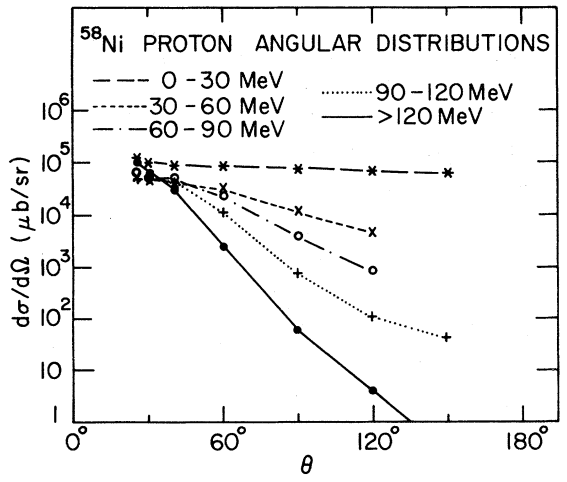

FIG. 6. Angular distributions in 30 MeV bins of the protons from a ^{58}Ni target.

With ^{62}Ni at 25° the deuteron spectrum falls off more rapidly with energy than does the proton spectrum. The triton and ^{3}He spectra show a still greater decrease with increasing exit particle energy. The evaporation peak is prominent in the proton spectrum, weaker but definitely present in the deuteron spectrum, but not strong enough to be clearly apparent in the triton and ^{3}He spectra. There is a prominent evaporation peak in the alpha spectrum which is broadened on the high side. While the lower portion of the peak was found to be nearly isotropic, the high side is strongly forward peaked. Above the low energy peak the alpha spectrum falls off more rapidly than do any of the others up to about 90 MeV. At higher energies the alpha spectrum appears to be somewhat flatter than the t or ^{3}He spectra, although the statistics in this region are quite poor for all three particles.

For the most part the spectra from the other targets showed similar variations with particle species. The triton data in Fig. 4 have been smoothed in order to facilitate comparison and it is clear that the shape of the spectra varies little with target. Similar statements could be made about the other species except that the broadening on the high energy side of the alpha evaporation peak was much greater for ^{208}Pb than for the lighter targets.

Angle integrated yields for producing the various particles are given in Table II. Also shown are the yields for energy $>$96 MeV, the top end of the spectrum, the yields for energy $>$30 MeV, an indication of the total number of fast particles of that type, and the area under the evaporation peak. The $>$30 MeV, $>$96 MeV, and total yields are from integrating the measured cross sections over the ob-

TABLE II. Angle integrated cross section in mb. The >30 MeV, >96 MeV, and total yields are integrated over the range $25° \leq \theta \leq 150°$, while the evaporation yield is over the entire sphere assuming an isotropic evaporation peak.

		Evaporation	>30 MeV	>96 MeV	Total
p	^{27}Al	147	250	82	460
	^{58}Ni	722	547	170	1427
	^{62}Ni	284	394	125	799
	^{208}Pb	78	797	236	1101
d	^{27}Al	14.5	21.6	3.9	49.2
	^{58}Ni	30.9	43.0	7.11	97.2
	^{62}Ni	25.9	36.4	5.76	80.2
	^{208}Pb	17.7	80.4	12.0	133.7
t	^{27}Al		1.9	0.17	8.0
	^{58}Ni		3.6	0.34	11.6
	^{62}Ni		4.0	0.30	15.7
	^{208}Pb		14.9	1.07	39.6
^{3}He	^{27}Al			0.06	4.5
	^{58}Ni		3.9	0.25	12.0
	^{62}Ni		2.3	0.08	5.8
	^{208}Pb		3.3	0.14	6.5
^{4}He	^{27}Al			0.27	29.7
	^{58}Ni	77	5.7	0.22	82.9
	^{62}Ni	57	4.5	0.41	65.9
	^{208}Pb	51	17.11	0.86	67.3

served angular range, while the evaporation yields were obtained by assuming isotropic evaporation peaks and integrating over the entire sphere. For the most part, the numbers given in Table II are believed to be accurate to about $\pm 15\%$ except where there were gaps in the spectra, as noted above. Thus, the cross sections for producing >30 MeV tritons from ^{27}Al, ^{62}Ni, and ^{208}Pb are uncertain to $\pm 25\%$ while the error for >30 MeV ^{3}He and ^{4}He from ^{62}Ni and ^{208}Pb is $\pm 50\%$. In addition, the aforementioned difficulty in defining the alpha evaporation peak from ^{208}Pb necessitates assigning it a $\pm 30\%$ error.

Another approach is to look at the yield of the more energetic of the various particles as a function of A. The fact that the relative yields from ^{58}Ni and ^{62}Ni are sometimes quite different (Table II) shows that detailed nuclear structure effects can be important, and thus only a rough A dependence can be determined. The deuteron yield varies with the atomic number of the target in much the same way that the proton yield does. However, the yield of fast tritons increases substantially more rapidly with A. In contrast, the fast ^{3}He yields do not show

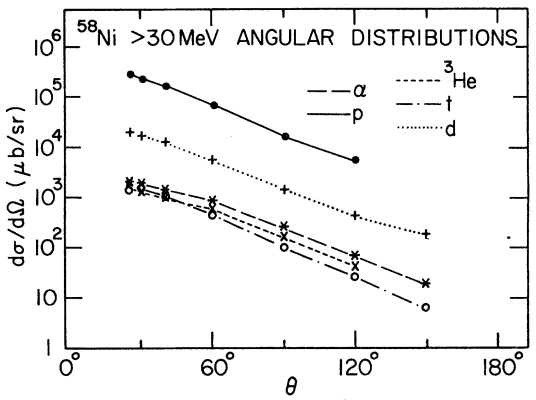

FIG. 7. Angular distributions of the fast (>30 MeV) portions of the spectra of the various exit particles. The target was ^{58}Ni.

a significant monotonic dependence of A (it should be noted that for ^{27}Al much of the region is missing for ^{3}He and ^{4}He). The behavior of the fast alpha yields is somewhere between that of tritons and ^{3}He.

The difference between the t and the ^{3}He behavior is quite striking. Between nickel and lead the fast triton yield increases by a factor of 3—4 while the fast ^{3}He yield does not change appreciably. Overall, the ratio of fast triton to ^{3}He production increases much faster than does the ratio of neutrons to protons in the nucleus.

As can be seen from Fig. 7, the angular distributions for the various particles are quite similar although there does seem to be some tendency for the more complex particles to be less forward peaked.

Figure 5 compares the 30° proton spectrum from ^{58}Ni at 100 MeV to that obtained at 164 MeV. The full energy peak, which includes inelastic scattering to low lying states as well as elastic scattering, is much larger at the lower energy. The shape of the continuum between the evaporation and the full energy peak is similar in the two spectra with the total number of protons in this region about 50% greater at the higher bombarding energy. Similar results were obtained with the other targets.

The shapes of the continua for the other particles

TABLE III. Inclusive cross sections at 30° for heavy ions from $p + ^{62}$Ni at 164 MeV.

Element	Cross section (μb/sr)
Li	55
Be	14
B	13
C	12
N	8
O	1.5

were also similar at the two bombarding energies. Figure 5 also shows the deuteron spectra for ^{62}Ni at 60°. The ratio of the yields of the various fast particles (i.e., >30 MeV $P:d:t:{}^3\mathrm{He}:\alpha$) was also about the same at the two bombarding energies. At the lower energy about 15% more fast protons (excluding the full energy peak) were found from ^{58}Ni than from ^{62}Ni.

Table III lists inclusive cross sections for heavy ions detected at 30° for the interaction of 164 MeV protons with ^{62}Ni. Cross sections decrease rapidly with the atomic number of the outgoing particle and essentially no particles heavier than oxygen were observed. Some of this decrease may result from the rapid rise with atomic number of the threshold energy for detection of these particles ($\sim$3 MeV for lithium and $\sim$24 MeV for oxygen), but it is at least clear that the production of fast heavy ions does not contribute substantially to the total reaction cross section.

IV. COMPARISON WITH CALCULATIONS

To date the only calculations that appear to be appropriate for intermediate energy reaction where a significant fraction of the incident particle's energy is given up are either cascade[8,9] or exciton[10] calculations. In a cascade calculation the incident particle enters the nucleus at a position chosen at random. It can then either pass through the nucleus or be scattered by a nucleon in the nucleus. If there is an interaction both the incident and the struck nucleon can either leave the nucleus or scatter again. The cascade continues until no nucleon has enough energy to escape. At each juncture the next event is chosen at random with probabilities determined from free nucleon-nucleon cross sections. Pauli blocking is allowed for by rejecting events where a nucleon would be promoted or demoted into an orbit that is already filled. Various embellishments can be made in the calculation but, as yet, it has not been possible to include complex particle formation.

Cascade calculations were done using the code VEGAS.[8,9] The neutron and proton distributions were taken to be the same, continuous, and of the form

$$\rho=\rho_0\frac{1}{1+e^{\frac{(i-c)}{a}}}$$

with the $c=1.05A^{1/3}$ fm and $a=0.56$ fm. The nucleons were assumed to have a Fermi momentum distribution which varies with the density.[9] Figure 8 shows the results of such a calculation along with the experimental data. Because the Monte Carlo calculations use a great deal of computer time, only a limited number of case histories can be calculated, in this case 30 000, and, therefore, the statistical fluctuations in the calculated spectrum are considerably greater than those in the experimental data.

The cascade calculations were found to at least qualitatively reproduce many of the features of the proton spectra, and were in good agreement with the measured shape of the angle integrated spectra. However, as can be seen in Fig. 8, the calculation predicts too prominent a quasifree peak. Furthermore, the calculation grossly underpredicts the number of fast protons at angles of 90° or more.

In the exciton model[10] the incident energy is dissipated by successively creating particle-hole pairs (excitons). States are characterized by the number of excitons and each state can emit nucleons as well as more complex particles. In order to calculate the complex particle, spectra formation factors, which may be excitation energy dependent, must be fed in for each particle. These formation factors are supposed to be obtained from reaction data but since such data are very scarce in this energy region, the formation factors used in the present calculations were, of necessity, quite arbitrary. The calculation is done in excitation energy space and all angular information is lost. Because the calculation does not predict the angular distribution, it is difficult to find a meaningful comparison of calculated with

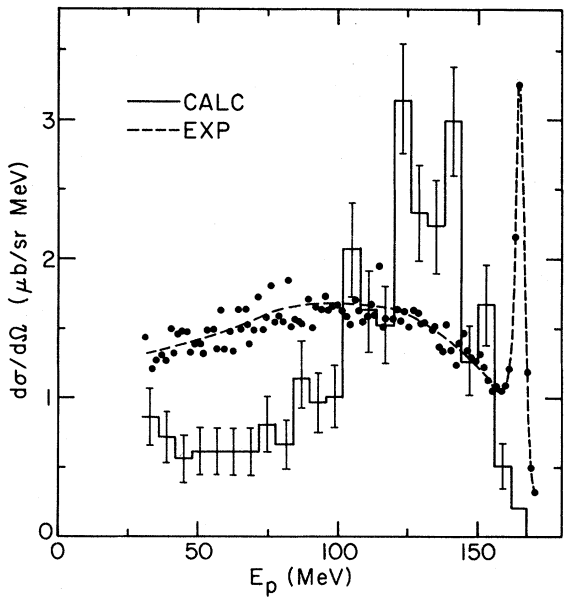

FIG. 8. Observed and calculated spectrum of protons from ^{62}Ni at 25°. The calculations were done using the Monte Carlo cascade code VEGAS.

observed spectra. The difficulty is that the calculation integrates over all angles while the experiment only went forward to 25°. Fast particles are strongly peaked forward, with the forward peaking increasing with exit particle energy and, therefore, a significant and varying fraction of particles were missed. Since there does not appear to be a reliable way to extrapolate into the unmeasured region, it is hard to meaningfully compare measured and calculated fast particle spectra. Nevertheless, some information as to the validity of the model could be extracted. For all these complex particles the calculations predict a smaller falloff with exit particle energy than is observed and, therefore, a larger cross section at the high energy end. These differences may, of course, be due to the fact that measurements were not made forward of 25°. However, the proton spectrum is predicted to decrease more rapidly with outgoing energy than does the deuteron spectrum, and this is in disagreement with experiment. The predicted proton spectrum actually is similar to the experimental spectrum integrated between 25° and 150° and therefore, discrepancies can be expected if measurements are carried out over the full angular range. It thus appears that the exciton calculations do not completely reproduce the trends in the data, at least so far as relating the proton data to that of the more complex particles and that, at any rate, the model is of limited use in predicting inclusive spectral measurements because the model requires integration over the entire angular range.

V. DISCUSSION OF RESULTS AND CONCLUSIONS

Protons are the dominant fast charged particle product, accounting for $>90\%$ of the fast charged particle yield. Protons are also the most evaporated charged particle, though for ^{208}Pb the proton and alpha evaporation yields are comparable. An important result deduced from the proton spectra is the weakness of the quasifree peaks.

The smearing out of the quasifree peak can be interpreted as indicating that the mean free path of the exiting nucleons is small compared to nuclear dimensions, resulting in considerable multiple scattering. Evidence that multiple scattering effects are important also comes from the variation of the shape of the proton spectra with target mass. There is a distinct indication of a quasifree peak in the proton spectrum from ^{27}Al at 25° while with ^{208}Pb the remnant of any such peak is all but gone. The fact that the fast proton yield increases more rapidly with A in the backward direction than in the forward direction can also be ascribed to multiple scattering.

The mean free path of nucleons in the nuclear medium is by no means well determined. Free nucleon-nucleon cross sections would lead to a mean free path of about 1.5 fm in this energy region (≈ 100 MeV). Pauli blocking, which is the suppression of interactions which would leave nucleons in states that are already filled, might be expected to increase this by as much as a factor of 2. Negele and Yazaki[12] have shown that if the nonlocality of the nuclear optical potential is properly taken into account, the theoretical nucleon mean free path is substantially increased and is about 4 fm at 150 MeV.

In terms of an optical model the mean free path can be linked directly to the imaginary part of the potential. In this sense, the mean free path has been experimentally determined to be about 5 fm in this energy region.[13] However, it has been shown[14] that the value of the imaginary part of the potential that is extracted from an analysis of elastic scattering data can be quite sensitive to the shape of the real potential. In fact, Meyer and Schwandt[14] find that when a shape of the real potential that they consider to be better theoretically justified than the usual Woods-Saxon form is used, an analysis of ^{40}Ca elastic scattering data yields a mean free path of about 2 fm. It should be noted that the cascade calculations predict too prominent a quasifree peak and too few protons in backward directions, both indicative of too long a mean free path. In contrast, the work of Negele and Yazaki[12] would indicate that the cascade calculation uses too short a mean free path.

In order to help interpret the present results, a simple calculation was performed in which the incident protons were assumed to be scattered by individual nucleons in the nucleus yielding an angular and energy distribution obtained by a Fermi gas calculation. Normalization was made by integrating over the nucleus and equating the resultant total cross section to the optical model value of the reaction cross section [800 mb for ^{62}Ni at $E_p = 164$ MeV (Ref. 15)]. The protons within the nucleus were assumed to be attenuated by a factor $e^{-x/\lambda}$ where x is the distance traveled and λ the mean free path. Taking the nucleus to be a uniform sphere, the intensity of the quasifree peak, at a given angle, was calculated as a function of λ. The maximum height of a possible quasifree peak in an observed spectrum was taken to be the maximum cross section in the region of the expected peak, and by comparing this

maximum with the calculated intensities, a minimum attenuation, or maximum mean free path, could be obtained. For ^{62}Ni at 25°, this turned out to be about 0.6 times the nuclear radius. Using this mean free path, the nuclear radius was taken to be that needed to reproduce the optical model cross section, which led to a radius of 5.5 fm for ^{62}Ni, which, in turn, yields an upper limit of 3.3 fm for the mean free path. Similar results were obtained for the other targets. Thus, within the framework of this simple picture, the present data appear to put an upper limit of about 3.5 on the mean free path, which is somewhat lower than the value predicted in this energy region by Negele and Yazaki. However, it is difficult to come to a definite conclusion until more realistic calculations can be made.

The pattern of mass 3:*d*:*p* production of $\approx$1:10:100 indicates that much of the complex particle production is through successive pickup. However, the alpha yield is approximately equal to that of mass 3. Because of their small binding energies, the deuterons, tritons, and ^{3}He can all be expected to have short mean free paths while the more stable alpha particles might be expected to travel further. Thus, more alpha particles would escape the nucleus, giving an increased yield. The picture of complex particle production by successive pickup is supported by the shapes of the spectra, which fall off more rapidly with energy the more complex the particle, and by the angular distributions, which are largely independent of particle species.

A strong isotope effect is present in the mass 3 spectra. For >96 MeV particles the ratio of ^{3}He to *t* production for ^{58}Ni is about 0.74, the highest by at least a factor of 2 for any of the targets, while for ^{62}Ni this ratio is lower by about a factor of 3. Because of their expected short mean free paths the number of fast *t* and ^{3}He are likely to be very dependent on the makeup of the nuclear surface. Thus, the mass 3 spectra indicate that the surface of ^{58}Ni is significantly more proton rich than the ^{62}Ni surface. For the ^{208}Pb target, at the upper end of the spectrum the ^{3}He:*t* ratio is about 1:8, while for ^{27}Al this ratio is about 1:3, a trend which is in accord which the notion that the composition of the nuclear surface is a dominant factor in determining this ratio.

As an initial, survey experiment, a number of things have been uncovered where further work may be fruitful. While quasifree scattering is certainly less important than previously believed, it would nevertheless be desirable to see if, at these energies, it becomes prominent at forward angles as it does at 800 MeV (Ref. 11) incident energy. The present spectra appear to require that $\approx$150 MeV protons have a mean free no greater than about 3.5 fm but better calculations are needed. Data between the 164 MeV of the present work and 800 MeV might prove helpful. Measurements of *t* and ^{3}He production appear to offer the possibility of studying the nuclear surface and other comparisons of neutron-rich and neutron-poor nuclei of similar atomic number could be made. Finally, the theories that are available appear to be woefully inadequate and, hopefully, the quantity and the quality of the data that are becoming available will stimulate new theoretical approaches.

ACKNOWLEDGMENTS

The authors wish to thank Dr. Lon Chen Liu for performing the cascade calculations and Dr. M. Sadler for helping in the early stages of the experiment. This work was supported in part by the National Science Foundation.

---

*Present address: Oak Industries, Crystal Lake, IL 60014.

†Present address: Schlumberger, Ltd., Houston, TX 77002.

[1]T. Chen, R. E. Segel, P. T. Debevec, J. Wiggins, P. P. Singh, and J. V. Maher, Phys. Lett. 103B, 192 (1981).

[2]N. S. Wall and P. R. Roos, Phys. Rev. 150, 811 (1966).

[3]J. M. Cameron, P. Kitching, R. H. McCamis, C. A. Miller, G. A. Moss, J. G. Rogers, G. Roy, A. W. Stetz, C. A. Goulding, and W. T. H. van Oers, Nucl. Instrum. Methods 143, 399 (1977).

[4]E. Lomon and H. Feshbach, Rev. Mod. Phys. 39, 611 (1967).

[5]J. R. Wu, C. C. Chang, and H. D. Holmgren, Phys. Rev. C 19, 698 (1979).

[6]E. J. Moniz, I. Sick, R. R. Whitney, J. R. Ficenec, R. D. Kephart, and W. P. Trower, Phys. Rev. Lett. 26, 445 (1971).

[7]S. M. Levenson, D. F. Geesaman, E. P. Colton, R. J. Holt, H. E. Jackson, J. P. Schiffer, J. R. Specht, K. E. Stephenson, B. Zeidman, R. E. Segel, P. A. M. Gram, and C. A. Goulding, Phys. Rev. Lett. 47, 479 (1981).

[8]K. Chen, Z. Fraenkel, G. Friedlander, J. R. Grover, J. M. Miller, and Y. Shimamoto, Phys. Rev. 166, 949

(1968).
[9]I. Dostrovsky, Z. Fraenkel, and G. Friedlander, Phys. Rev. 116, 683 (1959).
[10]M. Blann, Annu. Rev. Nucl. Sci. 25, 123 (1975).
[11]R. E. Chrien, T. J. Krieger, R. J. Sutter, M. Way, H. Palevsky, R. L. Stearns, T. Kozlowski, and T. Bauer, Phys. Rev. C 21, 1014 (1980).
[12]J. W. Negele and K. Yazaki, Phys. Rev. Lett. 47, 71 (1981).
[13]A. Nadasen, P. Schwandt, P. P. Singh, W. W. Jacobs, A. D. Bacher, P. T. Debevec, M. D. Kaitchuck, and J. T. Meek, Phys. Rev. C 23, 1023 (1981).
[14]H. O. Meyer and P. Schwandt, Phys. Lett. 107B, 353 (1981).
[15]M. E. Sadler, P. P. Singh, J. Jastzebski, L. L. Rutledge, Jr., and R. E. Segel, Phys. Rev. C 21, 2303 (1980).